**Biogeosciences
Discussions**

Biogeosciences Discussions is the access reviewed discussion forum of *Biogeosciences*

The fate of pelagic CaCO$_3$ production in a high CO$_2$ ocean: A model study

M. Gehlen[1], R. Gangstø[1], B. Schneider[1], L. Bopp[1], O. Aumont[2], and C. Ethe[1]

[1]LSCE/IPSL, Laboratoire des Sciences du Climat et de l'Environnement, CEA-CNRS-UVSQ, Orme des Merisiers, Bât. 712, CEA/Saclay, 91198 Gif-sur-Yvette Cedex, France
[2]LOCEAN/IPSL, Centre IRD de Bretagne, BP 70, 29280 Plouzané, France

Correspondence to: M. Gehlen (marion.gehlen@cea.fr)

EGU

M. Gehlen et al.

Abstract

This model study addresses the change in pelagic calcium carbonate production (CaCO$_3$, as calcite in the model) and dissolution in response to rising atmospheric CO$_2$. The parameterization of CaCO$_3$ production includes a dependency on the sat-
5 uration state of seawater with respect to calcite. It was derived from laboratory and mesocosm studies on particulate organic and inorganic carbon production in *Emiliania huxleyi* as a function of pCO$_2$. The model predicts values of CaCO$_3$ production and dissolution in line with recent estimates. The effect of rising pCO$_2$ on CaCO$_3$ production and dissolution was quantified by means of model simulations forced with atmospheric
10 CO$_2$ increasing at a rate of 1% per year from 286 ppm to 1144 ppm. The simulation predicts a decrease of CaCO$_3$ production by 27%. The combined change in production and dissolution of CaCO$_3$ yields an excess uptake of CO$_2$ from the atmosphere by the ocean of 5.9 GtC.

1 Introduction

15 About 50% of the CO$_2$ released by human activity since the beginning of the industrialization has accumulated in the atmosphere. The other half of the total release was taken up by the terrestrial biosphere (20%) and the ocean (30%). The world ocean is thus the largest sink for anthropogenic CO$_2$, with a total uptake of 118±19 Pg C between 1800 and 1994 (Sabine et al., 2004). In seawater CO$_2$ behaves like a weak
20 acid. The associated chemical reactions drive a decrease in pH (increase in acidity, decrease in alkalinity) and in carbonate ion concentration (CO$_2$ + H$_2$O + CO$_3^{2+}$ ↔ 2 HCO$_3^-$). This process known as acidification (e.g. Feely et al., 2004; Orr et al., 2005) decreases the saturation state of seawater with respect to calcium carbonate (CaCO$_3$). The saturation state is defined as the ratio of the in situ ion concentration

product $[Ca^{2+}]\times[CO_3^{2-}]$ over the stoichiometric solubility product Ksp (Mucci, 1983):

$$\Omega = \frac{\left[Ca^{2+}\right] \times \left[CO_3^{2-}\right]}{Ksp} \tag{1}$$

In the modern ocean, abiotic $CaCO_3$ precipitation is only a minor contribution to total carbonate production. The majority of $CaCO_3$ is produced by organisms: e.g. coralline algae (high-Mg calcite), pteropods, corals, bivalves (aragonite), coccolithophores (calcite), foraminifera (mostly calcite). The solubility decreases from high-Mg calcite, and aragonite to calcite, suggesting differing degrees of vulnerability of organisms to ocean acidification. Biogenic calcification takes place under supersaturated conditions. While the exact reaction pathway awaits further elucidation for most calcifiers, it has been shown that calcification strongly depends on the level of supersaturation. In general, calcification decreases with decreasing saturation state with a threshold value well above $\Omega=1$ (saturation). Unmitigated acidification of oceanic waters will ultimately threaten the existence of marine calcifiers and cause major changes in marine ecosystems.

In terms of feedback on rising atmospheric CO_2, three distinct yet interconnected groups of processes involving $CaCO_3$ can be identified:

1. Calcification: $CaCO_3$ precipitation leads to a pCO_2 increase according to Eq. (2):

$$Ca^{2+} + 2HCO_3^- \leftrightarrow CaCO_3 + CO_2 + H_2O \tag{2}$$

A decrease in calcification would thus favor the uptake of atmospheric CO_2 by the ocean and acts as a negative feedback on rising atmospheric pCO_2. A potential decrease of surface ocean pCO_2 of 10 to 20 μatm was estimated for a complete shutdown of surface ocean calcification (Gruber et al., 2004). The ratio of CO_2 released per mole of $CaCO_3$ precipitated (Ψ) is a function of the buffer capacity of the seawater acid-base CO_2 system. Under present conditions, roughly 0.6 moles of CO_2 are released per mole of $CaCO_3$ precipitated (Frankignoulle et al., 1994). This ratio is bound to increase

Pelagic $CaCO_3$ production in the future ocean

M. Gehlen et al.

Pelagic CaCO$_3$ production in the future ocean

M. Gehlen et al.

EGU

as the overall buffer capacity of seawater decreases in response to anthropogenic CO$_2$ uptake, thereby counteracting the effect of decreasing calcification.

2. Dissolution: The effect of dissolution follows directly from the stoichiometry of Eq. (2) (backward reaction). Enhanced dissolution of CaCO$_3$ in response to acidification increases upper ocean alkalinity thereby favoring CO$_2$ uptake, which can be considered as a negative feedback on atmospheric pCO$_2$.

3. CaCO$_3$ export and rain ratio effect: A decrease in calcification will alter the ratio of organic C to inorganic C (the rain ratio): an increase in rain ratio will promote the dissolution of CaCO$_3$ in marine sediments resulting in a higher alkalinity (Archer and Maier-Reimer, 1994), a negative feedback operating on timescales of 10 000 years. Alternatively, if the ratio of organic C to inorganic C is closely bound by the process of ballasting (Armstrong et al, 2002; Klaas and Archer, 2002), less CaCO$_3$ production would imply less ballasting of organic C (POC) fluxes and a shallower remineralization of POC which corresponds to a positive feedback.

The interplay between these processes makes it impossible to have an a priori knowledge of the amplitude and sign of the feedback associated with changes in the carbonate chemistry of seawater and calcification/dissolution/ballasting in response to ocean acidification. The present model study focuses on the response of calcification and CaCO$_3$ dissolution to rising pCO$_2$. The aim is, on one hand, to quantify the calcification/dissolution feedback on rising atmospheric CO$_2$, on the other, to quantify the relative sign and importance of individual processes.

2 Model description

2.1 The biogeochemical model PISCES: a brief general description.

The biogeochemical model PISCES (Aumont et al., 2003; Aumont and Bopp, 2006; Gehlen et al., 2006) simulates the biogeochemical cycle of oxygen, carbon and of the main nutrients controlling marine phytoplankton growth: nitrate and ammonium, phos-

phate, silicate and iron. The nutrient concentration is linked through a constant Redfield ratio and phytoplankton growth is limited by the external availability of nutrients. The cycles of carbon and nitrogen are decoupled in the model to a certain degree by nitrogen fixation and denitrification. The model distinguishes two phytoplankton size-classes
5 corresponding to nanophytoplankton and diatoms, and two zooplankton size classes which are microzooplankton and mesozooplankton. For all species, the C/N/P ratios are assumed constant. The prognostic variables of phytoplankton are total biomass, iron, chlorophyll and silicon contents. The internal ratios of Fe/C, Chl/C and Si/C of phytoplankton are predicted by the model. For zooplankton, the total biomass is the
10 only prognostic variable. The bacterial pool is not modeled explicitly. The model distinguishes three non-living compartments for organic carbon: semi- labile dissolved organic carbon (DOC) with timescales of several weeks to several years, two size classes of particulate organic carbon (small particles = POCs and big particles = POCb). While the C/N/P composition of dissolved and particulate matter is tied to Redfield stochiom-
15 etry, the iron, silicon and carbonate contents of the particles are diagnosed.

The two particulate detrital pools (POCs and POCb) are fueled by mortality, aggregation from nanophytoplankton and diatoms, fecal pellet production and grazing. Mineralization of particulate organic carbon together with excretion contributes to the semi-labile pool of dissolved organic carbon. Differential settling and turbulence pro-
20 mote particle aggregation. The parameterization of aggregation is based on Jackson (1990) and Kriest and Evans (1999, 2000). Small particles sink with a constant sinking speed of 3 m/d. Large particles, as well as $CaCO_3$ and SiO_2 sink with a sinking speed increasing with depth from 50 m/d at the base of the mixed layer to 200 m/d at 2000 m, respectively 425 m/d at 5000 m depth.

25 A detailed description of PISCES, including model equations and parameters is available as supplementary material in Aumont and Bopp (2006). We present hereafter a description of $CaCO_3$ production and dissolution. These parameterizations were adapted for the scope of the present study.

EGU

2.2 Biogeochemical cycle of carbonate in PISCES

PISCES simulates dissolved inorganic carbon and total alkalinity (carbonate alkalinity + borate + water). The carbon chemistry is computed following the OCMIP protocols (www.ipsl.jussieu.fr/OCMIP).

2.2.1 Carbonate production

Marine calcifiers are not implemented as a distinct plankton functional group in PISCES. In the model standard version, carbonate production is assigned to nanophytoplankton as a function of temperature and nutrient levels. Calcium carbonate is produced only as calcite. The bloom forming calcite producing coccolithophore *Emiliania huxleyi* is a prominent representative of calcifying nanophytoplankton. Parameter values controlling $CaCO_3$ production were chosen such as to reproduce the general distribution patterns of these coccolithophores (Moore et al., 2002; Aumont and Bopp, 2006). For the purpose of this study, the standard parameterization of $CaCO_3$ formation was updated to account for the saturation state of ambient waters with respect to calcite based on a synthesis of experimental studies.

Several studies have addressed the effect of increasing atmospheric pCO_2 on the production of calcite and the particulate inorganic carbon (PIC) to particulate organic carbon (POC) ratio in *E. huxleyi*. Experimental studies encompass laboratory experiments with monospecific cultures of *E. huxleyi* (Riebesell et al., 2000; Sciandra et al., 2003; Zondervan et al., 2001, 2002) and results from a mesocosm experiment with a natural phytoplankton population dominated by this calcifying species (Delille et al., 2005). All studies document a decrease in calcification with increasing pCO_2. The response in terms of the PIC to POC ratio is more differentiated and depends on light and nutrient conditions. Under N-limited growth conditions, Sciandra et al. (2003) report constant PIC to POC ratios for *E. huxleyi* cultures grown under elevated pCO_2. The constant PIC to POC ratio results from the concomitant decrease in inorganic carbon and organic carbon production. Experiments with nutrient replete *E. huxleyi*

Pelagic CaCO$_3$ production in the future ocean

M. Gehlen et al.

EGU

cultures (Riebesell et al., 2000; Zondervan et al., 2001, 2002), yielded to the contrary a decrease in PIC/POC with increasing pCO_2 resulting from the combined effect of a decrease in inorganic carbon production and an increase in organic carbon synthesis. The same response was found during a mesocosm experiment with a natural phyto-
5 plankton population dominated by blooming *E. huxleyi* (Delille et al., 2005).

We included only experimental data from N-replete experiments for the purpose of this model study (Delille et al., 2005; Riebesell et al., 2000; Zondervan et al., 2001, 2002). The saturation state of seawater with respect to calcite was computed from measured total alkalinity and pCO_2 using the CO2SYS Package (Lewis and Wallace,
10 1998). Experimental PIC to POC ratios are plotted as a function of undersaturation of seawater with respect to calcite (Ω_c) in Fig. 1. All experiments document a qualitatively similar response to a decrease in saturation state Ω_c (Fig. 1). The scatter in the data reflects differences in experimental conditions (f.i. nutrient availability and light conditions). Due to the limited number of observations, all data were used to derive
15 the parameterization describing the carbonate production as a function of Ω_c. Since the biocalcification underlies physiological controls, a Michaelis-Menten kinetic was selected for the dependency of the carbonate production - expressed as the ratio of PIC to POC - to the saturation state:

$$\frac{PIC}{POC} = \left(\frac{PIC}{POC}\right)_{max} \times \frac{(\Omega_{c-1})}{Kmax + (\Omega_{c-1})} \qquad (3)$$

20 where: PIC/POC = ratio of inorganic to organic carbon; $PIC/POC_{max} = 0.8$, maximum ratio observed under optimal growing conditions; Kmax = 0.4, with analogy to the half saturation constant, value of $(\Omega_c - 1)$ for which PIC/POC equals half of its maximal value.

The ratio PIC/POC max was chosen to equal 0.8. While in monospecific cultures
25 values up to 1 might be encountered, the ratio PIC to POC in natural phytoplankton population does not exceed 0.8 even when coccolithophores are blooming (see Fig. 1 and corresponding references). The value of Kmax of 0.4 reflects the observation that

Pelagic CaCO$_3$ production in the future ocean

M. Gehlen et al.

EGU

Pelagic CaCO₃ production in the future ocean

M. Gehlen et al.

for some marine calcifiers calcification decreases rapidly below a threshold value of Ω=4.0 (Gattuso et al., 1998).

Following the new parameterization, the model computes carbonate production as a function of environmental parameters (temperature, nutrient limitation and saturation state). We refer to this production as the *potential* $CaCO_3$ production. The pool of sinking carbonate particles is fueled by mortality and grazing on calcifying nanophytoplankton. Half of the grazed shells are routed to the sinking flux of $CaCO_3$, the other half is assumed to dissolve in the guts of grazers. The resulting carbonate flux corresponds to the *net* $CaCO_3$ production. This description was adopted in order to account for the observed, yet largely unexplained, loss of carbonate production in the upper ocean (Milliman et al., 1999).

2.2.2 Carbonate dissolution

Carbonate dissolution is described as a first order reaction with respect to undersaturation:

$$R_{DISS} = k \times (1 - \Omega_c) \tag{4}$$

We estimated the dissolution rate parameter k (1/time) from $CaCO_3$ fluxes recorded by sediment traps compiled into a comprehensive data base (Dittert et al., 2005; Gehlen et al, 2006). Particle sinking speed at depth of trap deployment was obtained from the model parameterization of sinking speed of large particles:

$$w = w_{min} + (w_{max} - w_{min}) \times \max\left(0, \frac{z - z_m}{2000}\right). \tag{5}$$

where: w_{min}, minimum sinking speed of 50 m/d; w_{max}, sinking speed at 2000 m below the mixed layer of 200 m/d; z, depth; z_m, depth of mixed layer.

From the $CaCO_3$ fluxes recorded at different depths along a trap mooring and knowing sinking speed, the fraction of $CaCO_3$ lost to dissolution was calculated.

$$F_z^{CaCO3} = F_{z+1}^{CaCO3} + F_{DISS} \tag{6}$$

where: F_z^{CaCO3}, flux of $CaCO_3$ at depth z (shallow trap), mol/m^2/d;

F_{z+1}^{CaCO3}, flux of $CaCO_3$ at depth z+1 (deeper trap), mol/m^2/d;

F_{DISS}, dissolution flux, mol/m^2/d.

This approach implies that lateral advection of particles can be neglected. The dis-
solution flux is then computed assuming the reaction kinetic of Eq. (4). The dissolution
rate parameter is obtained by fitting computed flux profiles to observed ones. We de-
termined an optimum fit value of 327 per month for the dissolution rate parameter k.
The flux of $CaCO_3$ reaching the last model box (=lower boundary) is re-dissolved in-
stantaneously after removing the alkalinity equivalent corresponding to river input. The
model is strictly mass conserving.

3 Methodology

The 3-D global ocean general circulation model OPA (Madec et al., 1998) provided
the physical forcing fields for tracer transport. After 3000 years of integration, modeled
nutrient and chlorophyll fields have reached a quasi steady-state with yearly mean
distributions and seasonal variations similar to observations (Aumont and Bopp, 2006).
The new parameterizations of carbonate production and dissolution were implemented
into the PISCES standard version and the model was run for another 400 years. This
allowed for a reorganization of dissolved inorganic carbon (DIC) and alkalinity (TALK)
fields down to 1000 m in response to the modified descriptions of calcification and
dissolution. Starting from the tracer distributions reached after 400 years, 3 model
experiments were performed with atmospheric pCO_2 increasing at a rate of 1% per
year from the pre-industrial level of 286 ppm to 4 times this value. In the first simulation,
calcification and dissolution depended on the saturation state of seawater with respect
to calcite. In the second experiment, calcification was independent of saturation state
(= constant at values corresponding to the initial state) and dissolution was allowed to
respond to changes in saturation driven by rising pCO_2. A third simulation was set up to

isolate the effect of the solubility pump by keeping $CaCO_3$ production and dissolution at preindustrial values. All three scenarios (labeled CAL01 to CAL03) were doubled with a corresponding control-run (labeled CTL01 to CTL03) at constant pCO_2. Table 1 summarizes model simulations carried out.

4 Results and discussion

4.1 The carbonate cycle in PISCES: Initial state

The global mean alkalinity profile is plotted in Fig. 2a. The model was initialized with the global mean alkalinity concentrations by Goyet et al. (2000). Mean concentrations profiles after Goyet et al. (2000) are included in Fig. 2 for comparison. The shape of modeled alkalinity profile corresponds reasonably well to the data. While the model yields slightly higher alkalinity levels in the upper 3000 m of the water column, deep water concentrations are underestimated. Figure 2b presents the depth of the calcite lysocline predicted by the model. The preindustrial ocean is characterized by a deep calcite lysocline in the Atlantic Ocean. In the North Atlantic the entire water column is oversaturated with respect to calcite. The lysocline shoals along the flow path of the overturning meridional circulation from North to South across the Atlantic and from South to North in the Pacific. Together with the model data comparison presented by Aumont and Bopp (2006), Fig. 2 emphasizes the capability of the model to reproduce the large scale distribution of biogeochemical tracers in the world ocean.

Global rates were computed for the potential, as well as the net carbonate production and dissolution. They are summarized and compared to literature results in Table 2. The potential $CaCO_3$ production of 1.3 PgC/yr includes the carbonate fraction lost to dissolution during zooplankton grazing. It corresponds to a gross production. In terms of CO_2 fluxes, the net production (0.8 PgC/yr) is the relevant quantity. It falls at the lower end of published estimates. The model predicts a global dissolution flux of 0.5 PgC/yr and compares well to the Feely et al. (2004) estimate. The $CaCO_3$ flux at

Pelagic CaCO$_3$ production in the future ocean

M. Gehlen et al.

⏮ | ⏭

◄ | ►

Back | Close

Full Screen / Esc

Printer-friendly Version

Interactive Discussion

EGU

the lower model boundary reflects the boundary conditions and its inherent criteria of mass conservation.

The evolution with depth of the $CaCO_3$ dissolution rate is plotted on Fig. 3 (a) for the Atlantic (black), Pacific (red) and Indian (green) Ocean. The differences in the evolution with depth of dissolution rates reflect the varying depth of saturation horizon for calcite (Fig. 3b) between ocean basins. Model derived dissolution rates are low compared to in situ dissolution rates summarized by Feely et al. (2004). These were estimated from alkalinity fields (excess alkalinity TA*, Feely et al., 2002) and combine dissolution of calcite and the more soluble carbonate mineral aragonite. Dissolution driven by the upward migration of the calcite and aragonite lysoclines in response to anthropogenic CO_2 invasion adds to the flux at shallow depth. The model, to the contrary, only simulates calcite and predicts zero dissolution above the calcite saturation horizon. Including shallow dissolving aragonite as a tracer would contribute to an improved representation of carbonate geochemistry in the model. On the other hand, alkalinity based estimates (Feely et al., 2002) do not account for transport processes in computing excess alkalinity, the latter being totally ascribed to dissolution. Mixing might however transport TA* from below the lysocline to shallow depth (Friis et al., 2006). While the occurrence of shallow carbonate dissolution is documented by independent evidence (e.g. Schiebel, 2002), its amount is likely to be overestimated by the TA* technique.

The depth attenuation of $CaCO_3$ fluxes provides an alternative approach to estimate dissolution rates. Feely et al. (2004) compiled data from several trap arrays and computed corresponding dissolution rates. They are smaller than *in situ* estimates reported in the same paper. Modeled dissolution rates fall within the range of trap derived ones (Feely et al., (2004). The use of sediment trap data has its own sets of caveats (e.g. over-/undertrapping due to turbulence especially for traps deployed at depths <1000 m; intrusion of swimmers, hypothesis of a 1D system etc). Below 1000 m the trapping efficiency of sediment traps is reported to be close to 1 (Yu et al., 2001). We selected only traps deployed at depths > 1000 m for our analysis. The dissolution rate parameter "k"

EGU

EGU

was derived from CaCO$_3$ flux attenuation profiles and is not a free model parameter. The dissolution rate is the product of the kinetic expression (Eq. 3) times the concentration of CaCO$_3$ particles. The average CaCO$_3$ concentration is plotted with depth in Fig. 3c. Feely et al. (2004) used the depth attenuation of CaCO$_3$ fluxes from a different set of trap deployments to derive bulk dissolution rates. The correspondence between modeled dissolution rates and these estimates suggests that the concentration of CaCO$_3$ particles predicted by the model is in the right order of magnitude. To summarize the preceding discussion, the version of the PISCES model just presented computes a carbonate budget within the range of published estimates.

4.2 Model experiments

Table 3 summarizes simulation results for CaCO$_3$ production, export and dissolution. The reference state of the model presented in the previous section will be referred to as CAL01-1×pCO$_2$ in the following discussion. Figure 4 presents the surface ocean saturation state with respect to calcite for preindustrial conditions and 4×pCO$_2$. The preindustrial ocean is characterized by $\Omega_c > 4$ prevailing between 45° S and 50° N, which corresponds according to our parameterization to optimal conditions for calcification. As expected, the model predicts a decrease in Ω_c for 4×pCO$_2$ with values < 4, suggesting suboptimal conditions for pelagic calcification in the majority of the surface ocean. Model results are presented for net CaCO$_3$ production and CaCO$_3$ dissolution rates integrated over the entire water column in Fig. 5. Net CaCO$_3$ production decreases in response to anthropogenic CO$_2$ invasion (Fig. 5b and c). The model predicts a decrease of total production at 2×pCO$_2$ from 0.79 to 0.74 PgC/yr, which further drops to 0.58 PgC/yr at 4×pCO$_2$ yielding a total decrease of 27%. At the same time, the CaCO$_3$ export flux at 100 m decreased by 29% over the course of experiment CAL01. The slightly higher decrease of export flux compared to calcification (27%) reflects the relative increase of dissolution.

The response of CaCO$_3$ dissolution to acidification of ocean waters is shown in Fig. 5d to f. Spatial patterns of Fig. 5e and f reflect bottom topography with increasing

dissolution along topographic heights (f.i. the mid-Atlantic ridge) and decreasing dissolution in the other areas. Since overall less carbonate particles are produced under rising atmospheric pCO_2, their complete dissolution will result in a lower absolute dissolution flux compared to the preindustrial state. This happens outside areas of benthic

5   $CaCO_3$ accumulation, where at $1\times pCO_2$ close to 100% of the carbonate flux gets dissolved before reaching the benthic boundary layer. In these areas, a shoaling of the lysocline will have little to zero impact on total dissolution. To the contrary, in regions with carbonate accumulation, a shoaling of the lysocline will result in an increase of the dissolution flux. Relative to total net production, dissolution increases from 61% at

10   $1\times pCO_2$ to 72% at $4\times pCO_2$.

    The decrease in calcification in CAL01 goes along with a relative decrease in surface water pCO_2, thereby increasing the capacity of the ocean for CO_2 uptake. An increase in pelagic $CaCO_3$dissolution is expected to further enhance this effect due to alkalinity production. However, the lower flux of carbonate particles translates in an overall lower

15   absolute dissolution flux (−16%), which partially counteracts the effect of decreasing production on air-sea CO_2 exchange. The combination of processes results in a net increase of the oceanic DIC inventory by 2.1%. In the experiment CAL02, where carbonate production was constant at preindustrial levels, we compute a net increase in dissolution of 19%. The effect of dissolution alone results in a DIC inventory increase

20   of the same order of magnitude as for CAL01. This result stresses the importance of changes in $CaCO_3$ dissolution in addition to production, in controlling the magnitude of the full $CaCO_3$ feedback on atmospheric CO_2 increase.

    Changes in DIC inventories computed for experiments CAL01 and CAL02 reflect the combined response of the solubility pump and $CaCO_3$ production and dissolution to

25   increasing atmospheric pCO_2. Experiment CAL03 during which carbonate production and dissolution were kept constant at pre-industrial levels allows the contribution of the solubility pump to be singled out. For experiment CAL01, both processes result in 5.6 GtC contributed less to the DIC inventory at the end of the simulation compared to CAL03. The uptake of CO_2 in the course of this simulation in excess to the sol-

Pelagic CaCO$_3$ production in the future ocean

M. Gehlen et al.

EGU

ubility pump is 5.9 GtC. In contrast with CAL01, constant calcification and increasing dissolution in CAL02 combine to a net contribution to the DIC inventory of + 3.1 GtC. To corresponding effect on alkalinity translates into an additional 1.2 GtC uptake as CO$_2$. Consequently, the effect of reduced calcification in CAL01 enhances the nega-
5   tive feedback to rising atmospheric CO$_2$ compared to CAL02, where only dissolution is at work. We computed an additional ocean uptake of CO$_2$ of 5.9 GtC at the end of experiment CAL01, driven by decreasing calcification and changing carbonate dissolution in response to acidification of surface waters. This effect is low compared to the total perturbation of about 750 GtC. It should however not preclude the expected
10   consequence for the entire pelagic ecosystem.

4.3   Comparison of assessments of future changes in marine calcification

Heinze (2004) predicts a global decrease in CaCO$_3$ of 50% at the end of a model experiment similar to CAL01. The final atmospheric CO$_2$ concentration was however higher than 4×pCO$_2$. At 4×pCO$_2$, carbonate production declined by approximately 38
15   % (Heinze, 2004; Fig. 3) compared to 27% in this study. While Heinze (2004) used different forcing scenarios, the discrepancy in the predicted sensitivity of calcification to acidification is most likely due to differences in the parameterizations of CaCO$_3$ production and its dependency on pCO$_2$. Heinze (2004) lets the CaCO$_3$ production be linearly dependent on seawater pCO$_2$. It is however likely that the biological response is
20   not linear with pCO$_2$, but rather follows an asymptotic type function. It is thus likely that Heinze (2004)'s estimate corresponds to an upper limit of the decrease of carbonate production in response to increasing pCO$_2$.
   Ridgwell et al. (2006) reach the opposite conclusion, namely that Heinze's (2004) estimate would be the lower limit of the expected response. They point to the poten-
25   tial bias introduced by parameterizations based on experimental results obtained for *Emiliania huxleyi*. Ridgwell et al. (2006) compiled experimental data documenting the calcification response of different organisms to increasing pCO$_2$. He fitted data from individual experiments (e.g. Bijma et al., 1999) or group of experiments (e.g. Zondervan

EGU

et al., 2001) to the widely accepted rate expression of $CaCO_3$ precipitation

$$R_{\text{PREC}} = k \times (1 - \Omega_c)^n. \tag{7}$$

Inorganic precipitation of calcium carbonate is known to follow Eq. (7) (Zhong and Mucci, 1993, and references therein). The reaction rate order n determined for inor-
ganic precipitation is strictly ≥ 1. Interestingly, with the exception of corals for which a value of $n \sim 1$ was determined, Ridgwell (2006) derived values of n ranging from 0.2 to 0.75 from biogenic calcification experiments. Previous studies (Hales and Emerson, 1997; Gehlen et al., 2005) highlighted potential sources of uncertainty in the determi-
nation of the reaction rate order from the reassessment of experimental data. Whether
values of $n < 1$ are a true characteristic of biotic calcification or an artifact introduced by fitting Eq. (7) to a limited set of scattered data needs further experimental elucidation.

The potential for a between species variability of the reaction of organisms to ocean acidification needs to be stressed. Langer et al. (2006) report data on the calcification response of the coccolithphores *Calcidiscus leptoporus* and *Coccolithus pelagicus* to
increased pCO_2. While to former displays an optimum curve centered at present day pCO_2, the later appears rather invariant to pCO_2 increase. Clearly, in order to improve our predictive capability of the impact of acidification on marine carbonate produc-
tion more experimental data are needed. This would also contribute to the necessary identification of reaction pathways for calcification in autotrophic and heterotrophic or-
ganisms.

5 Conclusions

The biogeochemical model PISCES was updated to include a dependency of $CaCO_3$ production on the saturation of seawater with respect to calcite and a revised param-
eterization of $CaCO_3$ dissolution. The model reproduces a marine carbonate cycle
largely consistent with independent estimates. The model underestimates $CaCO_3$ dis-
solution between 0 and 2000 m, which can in part be attributed to the fact that the

model only considers calcite.

Model experiments were carried out in order to quantify the evolution of $CaCO_3$ production and dissolution under conditions of increasing atmospheric CO_2. Carbonate production decreased by 27% in response to a pCO_2 increase of 1% per year from the preindustrial value of 286 ppm to $4 \times pCO_2$. Our study highlights the contribution of $CaCO_3$ dissolution to the feedback on increasing atmospheric pCO_2. Taken individually, the relative increase of dissolution in response to acidification drives an excess uptake of 3.1 GtC. The combined changes in $CaCO_3$ production and dissolution lead to an excess uptake of 5.9 GtC at the end of the simulation. Although this effect is low compared to the total perturbation of about 750 GtC, it should not hide the potential for major changes in ecosystem structure. The decrease in surface ocean saturation with respect to calcite threatens the competitiveness of pelagic calcifiers, among which *E. huxleyi* might be particularly vulnerable (Hendericks and Rickaby, 2006). A shift in species composition is likely to affect the entire food chain up to commercial fish. Associated changes in export production will modify the downward delivery of POC and thereby the availability of energy for the deep ocean and benthos.

References

Archer, D. and Maier-Reimer, E.: Effect of deep-sea sedimentary calcite preservation on atmospheric CO_2 concentration, Nature, 367, 2, 60–263, 1994.

Armstrong, R. A., Lee, C., Hedges, J. I., Honjo, S., and Wakeham, S. G.: A new, mechanistic model for organic carbon fluxes in the ocean: based on the quantitative association of POC with ballast minerals, Deep-Sea Res. II, 49, 219–236, 2002.

Aumont, O. and Bopp, L.: Globalizing results from ocean in situ iron fertilization studies, Global Biogeochem. Cy., 20, GB2017, doi:10.1029/2005GB002591, 2006.

Pelagic CaCO$_3$ production in the future ocean

M. Gehlen et al.

Title Page

Abstract | Introduction

Conclusions | References

Tables | Figures

◄ | ►

◄ | ►

Back | Close

Full Screen / Esc

Printer-friendly Version

Interactive Discussion

EGU

Aumont, O., Maier-Reimer, E., Blain, S., and Monfray, P.: An ecosystem model of the global ocean including Fe, Si, P colimitations, Global Biogeochem. Cy., 17(2), 1060, doi:10.1029/2001GB001745, 2003.

Bijma, J., Spero, H. J., and Lea, D. W.: Reassessing foraminiferal stable isotope geochemistry: Impact of the oceanic carbonate system (Experimental Results), in: Use of proxies in pale-oceanography: Examples from the South Atlantic, edited by: Fischer, G. and Wefer, G., 20 Springer-Verlag Berlin Heidelberg, pp. 489–512, 1999.

Bopp, L., Kohfield, K. E., Quéré, C. L., and Aumont, O.: Dust impact on marine biota and atmospheric pCO_2 during glacial periods, Paleoceanogr., 18(2), 1046, doi:10.1029/2002PA000810, 2003.

Delille, B., Harlay, J., Zondervan, I., Jacquet, S., Chou, L., Wollast, R., Bellerby, R. G. J., Frankignoulle, M., Borges, A. V., Riebesell, U., and Gattuso, J.-P.: Response of primary production and calcification to changes of pCO_2 during experimental blooms of the coccolithophorid Emiliania huxleyi, Global Biogeochem. Cy., 19, GB2023, doi:10.1029/2004GB002318, 2005.

Dittert, N., Corrin, L., Bakker, D., Bendtsen, J., Gehlen, M., Heinze, C., Maier-Reimer, E., Michalopoulos, P., Soetaert, K. E. R., and Tol, R. J. S.: Integrated Data Sets of the FP5 Research Project ORFOIS: Origin and fate of biogenic particle fluxes in the ocean and their interactions with atmospheric CO_2 concentrations as well as the amrine sediment (Vol. 1). WDC-MARE Reports 0002, 2005.

Feely, R. A., Sabine, C. L., Lee, K., Millero, F. J., Lamb, M. F., Greeley, D., Bullister, J. L., Key, R. M., Peng, T.-H., Kozyr, A., Ono, T., and Wong, C. S.: In situ calcium carbonate dissolution in the Pacific Ocean, Global Biogeochem. Cy., 16(4), 1144, doi:10.1029/2002GB001866, 2002.

Feely, A., Sabine, C. L., Lee, K., Berelson, W., Kleypas, J., Fabry, V. J., and Millero, F. J.: Impact of Antropogenic CO_2 on the $CaCO_3$ System in the Oceans, Science, 305, 362–366, 2004.

Frankignoulle, M., Canon, C., and Gattuso, J.-P.: Marine calcification as a source of carbon dioxide: Positive feedback of increasing atmospheric CO_2, Limnol. Oceanogr., 39(2), 458–462, 1994.

Friis, K., Najjar, R. G., Follows, M. J., and Dutkiewicz, S.: Possible overestimation of shallow-depth calcium carbonate dissolution in the ocean, Global Biogeochem. Cy., 20, GB4019, doi:10.1029/2006GB002727, 2006.

Gattuso J-P, Frankignoulle, M., Bourge, I., Romaine, S., and Buddemeier, R. W.: Effect of cal-

EGU

cium carbonate saturation of seawater on coral calcification, Global and Planetary Change, 18, 37–46, 1998.

Gehlen, M., Bassinot, F. C., Chou, L. and McCorkle, D.: Reassessing the dissolution of marine carbonates : I. Solubility. Deep Sea Research I 52(8), 1445–1460, doi:10.1016/j.dsr.2005.03.010, 2005.

Gehlen, M., Bopp, L., Emprin, N., Aumont, O., Heinze, C., and Ragueneau, O.: Reconciling surface ocean productivity, export fluxes and sediment composition in a global biogeochemical ocean model, Biogeosciences, 3, 521–537, 2006, http://www.biogeosciences.net/3/521/2006/.

Goyet, C., Healy, R., and Ryan, J.: Global distribution of total inorganic carbon and total alkalinity below the deepest winter mixed layer depths. (Carbon Dioxide Information Analysis Center, Oak Ridge National Laboratory, US Department of Energy, Tennessee), 2000.

Gruber, N., Friedlingstein, P., Field, C. B., Valentini, R., Heimann, M., Richey, J. E., Romero-Lankao, P., Schulze, D., and Chen, C.-T. A.: The vulnerability of the carbon cycle in the 21st century: An assessment of carbon-climate-human interactions, in: The Global Carbon Cycle: Integrating Humans, Climate, and the Natural World, Edited by: C. B. Field and M. R. Raupach, Island Press, Washington, D.C., 45–76, 2004.

Hales, B. and Emerson, S.: Evidence in support of first-order dissolution kinetics of calcite in seawater, Earth Planet Sc. Lett., 148, 317–327, 1997.

Henderiks, J. and Rickaby, R. E. M.: Algal constraints on the Cenozoic history of atmospheric CO_2?, Biogeosciences Discuss., 4, 1–11, 2007, http://www.biogeosciences-discuss.net/4/1/2007/.

Heinze, C.: Simulating oceanic CaCO3 export production in the greenhouse, Geophys. Res. Let., L16308, doi:10 1029/2004GL020613, 2004.

Iglesias-Rodriguez, M. D., Armstrong, R., Feely, R., Hood, R., Kleypas, J., Milliman, J. D., Sabine, C., and Sarmiento, J.: EOS, 83(34), 365, 2002.

Jackson, G. A.: A model for the formation of marine algal flocs by physical coagulation processes, Deep Sea Res., 37, 1197–1211, 1990.

Klaas, C., and Archer, D. E.: Association of sinking organic matter with various types of mineral ballast in the deep sea: Implications for the rain ratio, Global Biogeochem. Cy., 16(4), 1116, doi:10.1029/2001GB001765, 2002.

Kriest, I. and Evans, G. T.: Representing phytoplankton aggregates in biogeochemical models. Deep Sea Res. I, 46, 1841–1859, 1999.

Pelagic CaCO$_3$ production in the future ocean

M. Gehlen et al.

EGU

Kriest, I., and Evans, G.T.: A vertically resolved model for phytoplankton aggregation, Proc. Indian Acad. Sci. Earth Planet. Sci., 109, 453–469, 2000.

Langer G., Geisen, M., Baumann, K.-H., Kläs, J., Riebesell, U., Thoms, S., Young, J. R.: Species-specific responses of calcifying algae to changing seawater carbonate chemistry, Geochem. Geophys. Geosyst., 7, Q09006, doi:10.1029/2005GC001227, 2006.

Lee, K.: Global net community production estimated from the annual cycle of surface water total dissolved inorganic carbon, Limnol. Oceanogr., 46(6),1287–1297, 2001.

Lewis, E. and Wallace, D. W. R.: Program Developed for CO_2 System Calculations. ORNL/CDIAC-105. (Carbon Dioxide Information Analysis Center, Oak Ridge National Laboratory, US Department of Energy, Tennessee), 1998.

Madec, G. P., Delecluse, P., Imbard, M., and Lévy, C.: OPA 8.1 Ocean general circulation model reference manual, Notes du pole de modélisation, IPSL, 1998.

Milliman, J. D., Troy, P. J., Balch, W. M., Adams, A. K., Li, Y.-H., and Mackenzie F. T.: Biologically mediated dissolution of calcium carbonate above the chemical lysocline?, Deep-Sea Research I, 46, 1653–1669, 1999.

Moore, J. K., Doney, S. C., Kleypas, J. A., Glover, D. M., and Fung, I. Y.: An intermediate complexity marine ecosystem model for the global domain, Deep-Sea Research II, 49, 403–462, 2002.

Mucci, A.: The solubility of calcite and aragonite in seawater at various salinities, temperatures and one atmosphere total pressure, Amer. J. Sci., 283, 780–799, 1983.

Orr, J. C., Fabry, V. J., Aumont, O., Bopp, L., Doney, S. C., Feely, R. A., Gnanadesikan, A., Gruber, N., Ishida, A., Joos, F., Key, R. M., Lindsay, K., Maier-Reimer, E., Matear, R., Monfray, P., Mouchet, A., Najjar, R. G., Plattner, G.-K., Rodgers, K. B., Sabine, C. L., Sarmiento, J. L., Schlitzer, R., Slater, R. D., Totterdell, I. J., Weirig, M.-F. , Yamanaka, Y., and Yool, A.: Antropogenic ocean acidification over the twenty-first century and its impact on calcifying organisms, Nature, 437, 681–686, 2005.

Ridgwell, A., Zondervan, I., Hargreaves, J. C., Bijma, J., and Lenton, T. M. : Significant long-term increase of fossil fuel CO_2 uptake from reduced marine calcification, Biogeosciences Discuss., 3, 1763–1780, 2006,
http://www.biogeosciences-discuss.net/3/1763/2006/.

Riebesell, U., Zondervan, I., Rost, B., Tortell, P. D., Zeebe, R. E., and Morel, F. M. M.: Reduced calcification of marine plankton in response to increased atmospheric CO_2, Nature, 407, 364–368, 2000.

Pelagic CaCO$_3$ production in the future ocean

M. Gehlen et al.

EGU

Sabine, C. L., Feely, R. A., Gruber, N., Key, R. M., Lee, K., Bullister, J. L., Wanninkhof, R., Wong, C. S., Wallace, D. W. R., Tilbrook, B., Millero, F. J., Peng, T.-H., Kozyr, A., Ono, T., and Rios, A. F.: The oceanic sink for anthropogenic CO_2 Science, 3005, 367–370, 2004.

Schiebel, R.: Planktic foraminiferal sedimentation and the marine calcite budget, Global Biogeochem. Cy., 16, 1065, doi:10.1029/2001GB001459, 2002.

Sciandra, A., Harlay, J., Lefèvre, D., Lemée, R., Rimmelin, P., Denis, M., and Gattuso, J.-P.: Response of coccolithophorid *Emiliania huxleyi* to elevated partial pressure of CO_2 under nitrogen limitation, Mar. Ecol. Prog. Ser., 261, 111–122, 2003.

Zhong, S. J. and Mucci, A.: Calcite precipitation in seawater using a constant addition technique – a new overall reaction kinetic expression, Geochim. Cosmochim. Acta, 57, 1409–1417, 1993.

Zondervan, I., Zeebe, R. E., Rost, B., and Riebesell, U.: Decreasing marine biogenic calcification: A negative feedback on rising atmospheric pCO_2, Global Biogeochem. Cy., 15, 2, 507–516, 2001.

Zondervan, I., Rost, B., and Riebesell, U.: Effect of CO_2 concentration on the PIC/POC ratio in the coccolithophore Emiliania huxleyi grown under light-limiting conditions and different daylengths, J. Exp. Mar. Biol. Ecol., 272, 55–70, 2002.

Pelagic CaCO₃ production in the future ocean

M. Gehlen et al.

EGU

EGU

Table 1. Summary of simulations characteristics.

RUN ID	pCO$_2$ increase	CaCO$_3$ production dependent on Ω_c	CaCO$_3$ dissolution dependent on Ω_c
CAL01	yes	yes	yes
CTL01	no	yes	yes
CAL02	yes	cst at preind. level	yes
CTL02	no	cst at preind. level	yes
CAL03	yes	cst at preind. level	cst at preind. level
CTL03	no	cst at preind. level	cst at preind. level

Table 2. The carbonate cycle in PISCES: Comparison between model ouput and data. All fluxes (production, dissolution) are in Pg CaCO$_3$-C/yr.

Process	Model	Data	Data reference
Potential CaCO$_3$ production	1.3		
Net CaCO$_3$ production	0.8	0.8–1.4	Igelias-Rodriguez et al. (2002); Lee (2001)
Pelagic CaCO$_3$ dissolution	0.5	0.5	Feely et al. (2004)
CaCO$_3$ flux at lower boundary	0.3[1]	0.3[2]	Feely et al. (2004)

[1] model lower boundary conditions; [2] sediment accumulation;

Pelagic CaCO$_3$ production in the future ocean

M. Gehlen et al.

EGU

Table 3. Summary of results. Model output is presented in absolute numbers for and as % change for experiment CAL01-1×pCO$_2$. For all experiments, model output is given as drift corrected % change at 4×pCO$_2$ relative to the control simulation at constant pCO$_2$.

Process	CAL01-1×pCO$_2$	CAL01-2×pCO$_2$	CAL01-4×pCO$_2$	% change CAL01	% change CAL02	% change CAL03
Net CaCO$_3$ production (Pg C/yr)	0.79	0.74	0.58	−27	0	0
CaCO$_3$ export 100 m (Pg C/yr)	0.59	0.55	0.42	−29	−3.6	0
Pelagic dissolution (Pg C/yr)	0.48	0.46	0.42	−16	+19	0

EGU
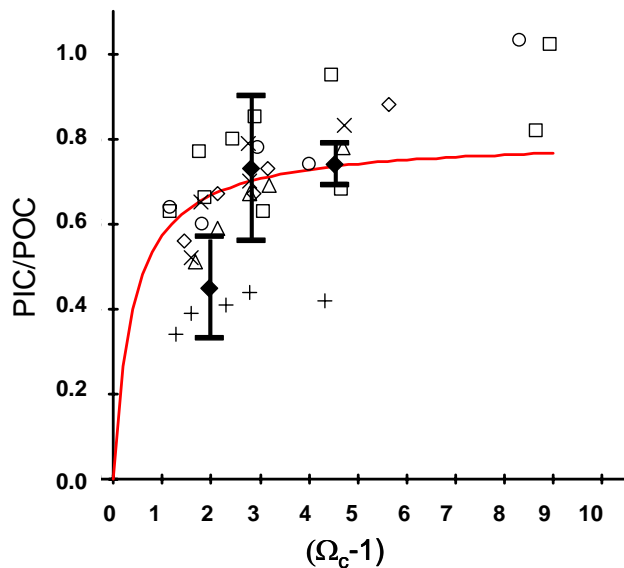
Fig. 1. The PIC/POC ratio as a function of the saturation state with respect to calcite, Ω_c. Open symbols, data by Zondervan et al. (2002). Closed diamonds, data by Delille et al. (2003). Solid line fit, obtained with Eq. (3).

M. Gehlen et al.

EGU

Calcite lysocline depth
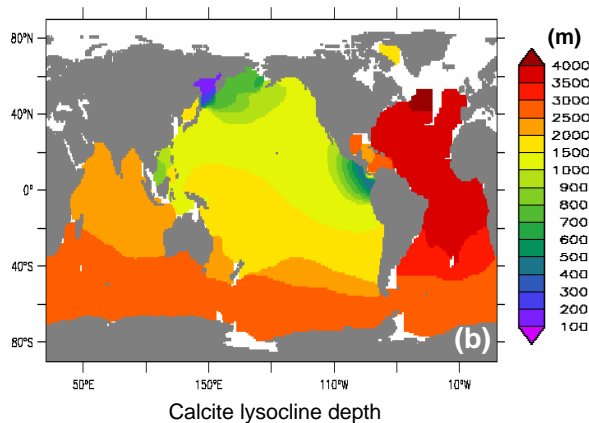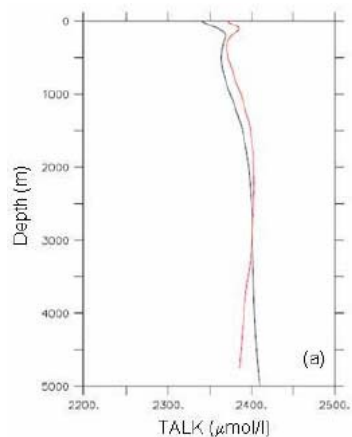
Fig. 2. (a) Mean global profiles of alkalinity in μmol/l. BLACK line = after Goyet et al. (2000),
RED line = model output. **(b)** Depth of calcite lysocline (m).
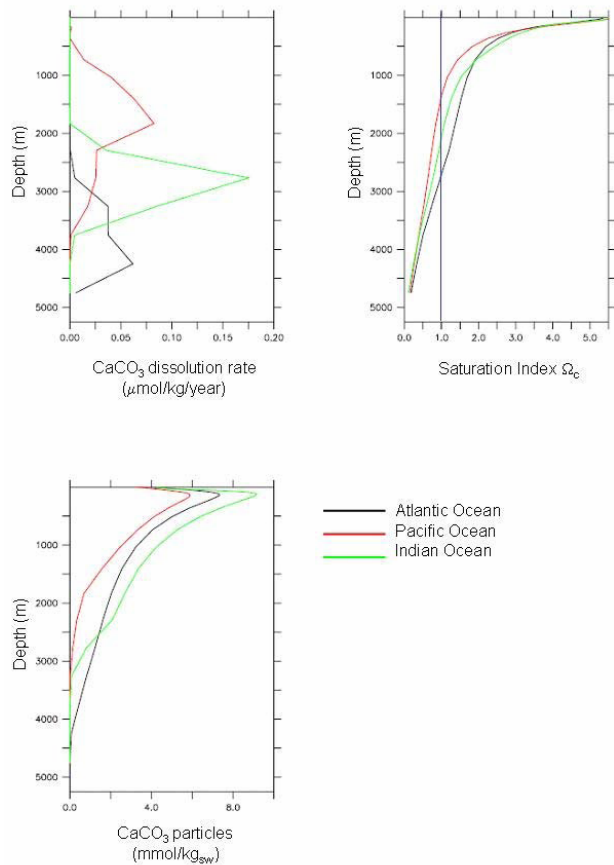
Fig. 3. **(a)** Average CaCO₃ dissolution rates; **(b)** Saturation index with respect to calcite; **(c)** mean concentration of CaCO₃ particles.

EGU

Title Page

Abstract | Introduction

Conclusions | References

Tables | Figures

◄◄ | ►►

◄ | ►

Back | Close

Full Screen / Esc

Printer-friendly Version

Interactive Discussion

EGU

Ω_c (0 – 100 m)

(a)

1 × pCO$_2$

Ω_c

(b)
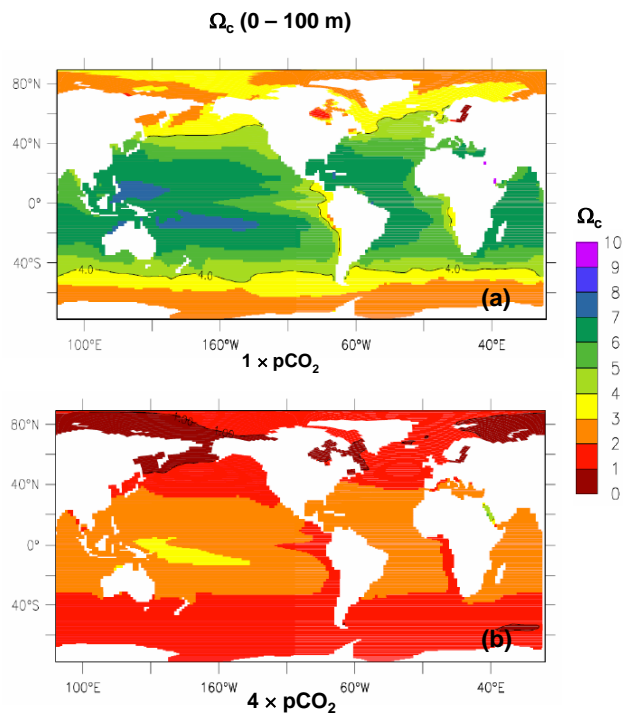
4 × pCO$_2$

Fig. 4. Saturation state Ω_c of surface ocean (0–100 m): **(a)** 1×pCO$_2$ and **(b)** 4×pCO$_2$.
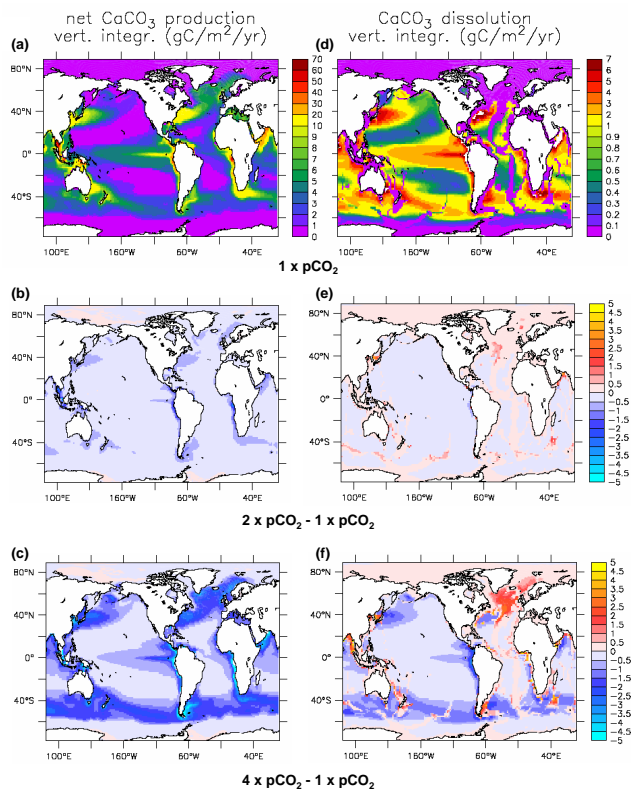
Fig. 5. Net CaCO$_3$ production and CaCO$_3$ dissolution in the simulation CAL01. **(a)** Vertical integrated net production (gC/m^2/yr) at 1×pCO$_2$; **(b)** difference in net production at 2×pCO$_2$ minus 1×pCO$_2$; **(c)** difference in net production at 4×pCO$_2$ minus 1×pCO$_2$; **(d)** vertical integrated dissolution rate (gC/m^2/yr) at 1×pCO$_2$; **(e)** difference in dissolution rate at 2×pCO$_2$ minus 1×pCO$_2$; **(f)** difference in dissolution rate at 4×pCO$_2$ minus 1×pCO$_2$.